Int. J. Electrochem. Sci., 15**(2020)** 5058 – 5066, doi: 10.20964/2020.06.84

International Journal of ELECTROCHEMICAL SCIENCE
www.electrochemsci.org

Rapid and sensitive detection of methotrexate using acetylene black electrode

Ziwen Deng, Qingwu Tian, YinghuaXu, LiminLun, SukaiSun, Xiaomin Yang, Ruhua Liu, Yusun Zhou, Hui Li[*,1]*, Tingting Zhou*[*,1]

Department of Clinical Laboratory, The Affiliated Hospital of Qingdao University,#16, Jiangsu Road, Qingdao, Shandong, 266003, China
[*]E-mail: lh99007@163.com, zhouting81205@163.com
[1]These authors equally contributed to this work

Received: 5 February 2020/ *Accepted:* 30 March 2020 / *Published:* 10 May 2020

A glassy carbon electrode sensor modified with acetylene black (AB) film was fabricated and successfully used in detecting methotrexate (MTX) in real clinical samples. In this study, a homogeneous suspension was obtained by ultrasonically dispersing AB into water for 1 h. The performance of the prepared sensor was studied via cyclic voltammetry. The prepared electrochemical sensor exhibited a good linear relationship within the range of 0.005 μM to 3.0 μM, and the detection limit for MTX was 3.81 nM. The sensor also demonstrated satisfactory selectivity, repeatability, and stability for MTX determination. Thus, a practical platform for detecting MTX in clinical samples is proposed.

Keywords: Methotrexate; Acetylene black; Electrochemical sensor

1. INTRODUCTION

Methotrexate (MTX), an important anti-metabolic agent, is widely used in treating acute leukemia and many types of cancer and autoimmune diseases [1-5]. However, this compound can cause several side-effects, such as gastrointestinal disorders, renal disease, myelosuppression, and seizure [5]. Studies have shown that MTX may increase the risk of male infertility and cause fetal malformation [6,7]. Therefore, after the infusion of high MTX dosage, calcium leucovorin can be administered to reduce the toxic side effects of MTX [8]. To effectively improve the safety of drug usage, the rapid and accurate determination of MTX concentration for the timely use of a rescue agent is highly significant.

Various methods, such as liquid chromatography–tandem mass spectrometry [9,10], high-performance liquid chromatography [11-13], and flow-through biosensor [14], have been reported for determining MTX. Although these methods have been successfully used in detecting MTX, their applications are limited by high cost and complex operation [15,16]. Therefore, a rapid, simple, and

economical method for MTX determination should be established. Electrochemical methods have elicited considerable interest because of their high sensitivity, good selectivity, low cost, and time-saving process [17].

However, in accordance with our experimental results, a bare glassy carbon electrode (GCE) cannot produce the ideal effect for detecting MTX. The chemical modification of the electrode's surface can provide the necessary absorbability and selectivity [16]. Acetylene black (AB), which is a special carbon black, has received considerable attention because of its excellent performance in electrical conductivity, surface activity, and other chemical properties [18,19]. Thus, AB exhibits superior electrochemical performance in determining various substances, such as chrysophanol, topotecan, erythromycin, and honokiol [20-23]. To our knowledge, AB has never been used to modify an electrode for MTX detection. In the current study, AB was introduced to modify a GCE, which was then successfully used in determining MTX in real clinical serum samples.

2. MATERIALS AND METHODS

2.1. Reagents

MTX was obtained from Macklin Biochemical Co., Ltd. (Shanghai, China). Glycine, glucose, and citric acid were purchased from Solarbio (Beijing, China). Vitamin C, zinc sulfate, sodium chloride, potassium chloride, ferric chloride, and potassium ferrocyanide were supplied by Sinopharm Chemical Reagent Co., Ltd. (Shanghai, China). AB was obtained from Brinway Biotechnology Co., Ltd. (Shanghai, China). MTX solution (0.1 mM) was prepared by dissolving MTX into methanol. Phosphate-buffered saline (PBS) of different pH values (0.1 M) was prepared with $Na_2HPO_4 \cdot 12H_2O$ and $NaH_2PO_4 \cdot 2H_2O$. Hydrochloric acid and sodium hydroxide were applied to adjust the pH of PBS. Distilled water was used throughout the experiment.

2.2. Instruments

A CHI660C electrochemical workstation was used (Shanghai Chenghua Apparatus, Shanghai, China). The three-electrode system was composed of AB/GCE, platinum electrode, and saturated calomel electrode. Model 901 intelligent magnetic stirrer was purchased from San-Xin Instrumentation, Inc. (Shanghai, China). PHS-25 pH meter was obtained from INESA Scientific Instrument Co., Ltd. (Shanghai, China).

2.3. Preparation of modified electrode

First, 2.0 mg of AB was added to 2.0 mL of water and dispersed ultrasonically for 1 h to obtain a fine homogeneous black suspension. Then, polishing powder was used to polish the GCE. Subsequently, the electrode was ultrasonically cleaned in absolute ethyl alcohol and water for 2 min in

sequence, until the electrode was as smooth as a mirror. Lastly, 4.5 μL of the AB dispersion solution was dropped onto the surface of the GCE and dried to obtain the AB/GCE.

2.4. Detection method

PBS (0.1 M, pH6.0) was selected as the electrolyte solution for MTX. Then, 50 μL of MTX (0.1 mM) was added to the electrolyte solution. Subsequently, the solution was stirred for 4 min, and cyclic voltammetry (CV) from 0.30 V to 1 V was recorded at a scan rate of 100 mV s^{-1}.

2.5. Sample preparation

The prepared electrode was used to detect MTX in the human serum to verify its feasibility for application in real samples. The sample should be deproteinized prior to electrochemical detection to eliminate the interference of various complex factors in the serum. Thereafter, 20 μL of the purified samples were diluted to 10 mL with PBS solution (0.1 M, pH6.0). Three types of MTX standard solutions with different concentrations (0.05, 0.1, and 0.2 μM) were added to the diluted samples for the recovery experiment.

3. RESULTS AND DISCUSSION

3.1. Electrochemical behavior of MTX

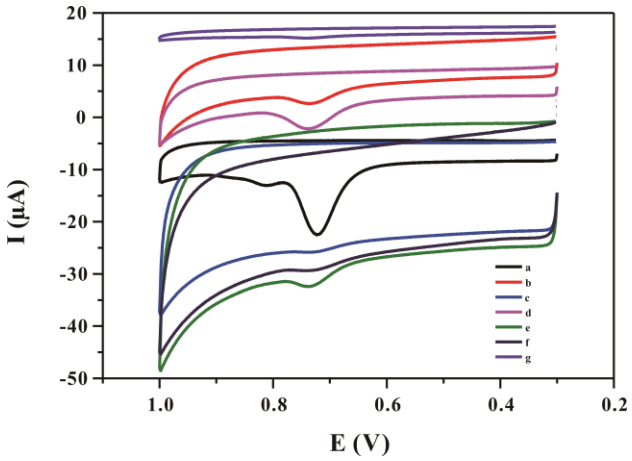

Figure 1. Effects of different types of catalytic materials on the oxidation peak current of 0.5 μM MTX. AB (a), single-layer carbon nano angle (b), carboxyl carbon tube (c), N-doped carbon nanotube (d), amino carbon tube (e), grapheme (f), and bare GCE (g). Scanning rate: 80 mV s^{-1}.

To select the best electrochemical materials for the adsorption and catalysis of MTX, we performed a series of experiments on the adsorption of MTX with different materials in 0.1 M phosphate buffer (pH6.0) via CV. The results are presented in Fig.1. As shown in the figure, the significant

oxidation peak of MTX appeared at 0.74 V, but no reduction peak was observed in reverse scanning. After the modification of the different materials, the peak oxidation value increased in different degrees. Compared with other materials modified electrodes, the AB-modified electrode exhibited the best adsorption and catalysis capacity. This result indicated the feasibility of this experiment, which was primarily attributed to the adsorption of MTX onto AB [24-26]. Although the substances detected were not exactly the same, the adsorption performance of AB in this process was beyond doubt in these papers. The AB-modified electrode might adsorb MTX via hydrophobic action and accelerated the oxidation of the target drug [24]. In addition, the amino group at C2 position on the pyrimidine ring of MTX is electrically active and easy to be catalyzed to form n-nitrogen radical intermediates [28]. The formation of insoluble products on the surface of the electrode by radical polymerization might also be one of the factors contributing to the increase of peak current.

3.2. Optimization of electrochemical experimental parameters

3.2.1. Effect of the amount of AB dispersion on MTX detection

The amount of AB as the core material in this experiment can affect the peak current value of MTX.

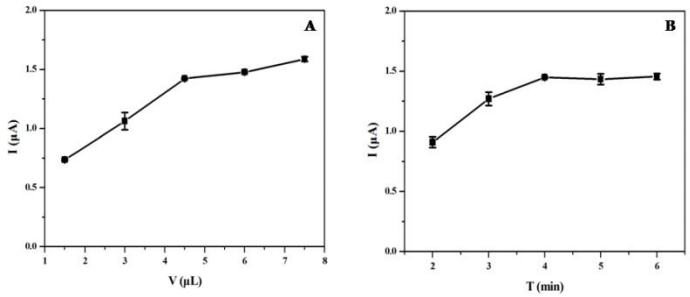

Figure 2. Effects of the amount of AB dispersion solution (A) and enrichment time (B) on the oxidation peak current of 0.1 μM MTX in PBS (0.1 M, pH6.0). Scanning rate: 80 mV s^{-1}.

Fig.2A shows that the peak current value of MTX at the AB-modified electrode significantly increased with an increase in the volume of the AB dispersion solution from 1.5 μL to 4.5 μL. When the volume of the AB dispersion solution was further increased to 7.5 μL, the current value of MTX slowly increased. Meanwhile, the increase in the volume of the AB dispersion solution can increase the baseline of the CV curve. Considering the aforementioned factors and cost-saving, the optimum volume of the AB dispersion solution was 4.5 μL.

3.2.2. Effect of MTX enrichment time on detection

The effect of enrichment time on the current response was examined from 2 min to 6 min. As shown in Fig.2B, the peak current before 4 min was proportional to the enrichment time, but the correlation weakened thereafter. The results showed the highest adsorption efficiency of MTX at an enrichment time of 4 min.

3.2.3. Effects of buffer pH and scan rate on MTX detection

The effect of buffer pH on MTX peak current was investigated by varying pH level from 3.6 to 8.0 at a scan rate of 80 mVs^{-1}. As shown in Fig.3A, a prominent increase in peak current was observed from 3.6 to 6.0. Then, the oxidation peak current of MTX decreased in the pH range from 6.0 to 8.0.

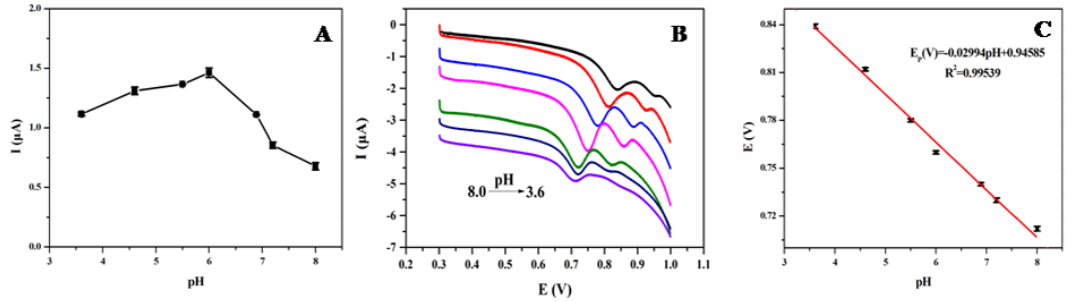

Figure 3. (A) Effects of buffer pH on peak current. (B) CV curve of 0.1 μM MTX in PBS (0.1 M, pH6.0) on AB/GCE at different pH levels of 3.6, 4.6, 5.5, 6.0, 6.9, 7.2, and 8.0. (C) Linear relationship of peak potential and buffer pH. The other conditions are the same as those in Fig.2.

Therefore, 6.0 was the optimal pH level. In addition, the peak oxidation potential of MTX gradually shifted negatively with an increase in pH value within the range of 3.0 to 8.0 (Fig.3B). As shown in Fig.3C, the peak oxidation potential of MTX was negatively linearly correlated with the pH value from 3.0 to 8.0, and the linear equation was calculated to be E_P (V)= -0.02994pH+0.94585 (R^2=0.99539). The obtained slope (−29.94 mV) was nearly half of the theoretical value of Nernst's equation (−59 mV), indicating that the number of electrons involved in the MTX oxidation was two times that of protons.

In this study, the electrochemical performance of the prepared sensor was discussed though CV. In addition to buffer pH, the effect of scan rate on the results should not be disregarded (Fig.4A). As shown in Fig.4B, the peak oxidation current of MTX was proportional to the scan rate, and the linear equation was I (μA)= 0.02016v+0.06163 (R^2=0.99912). This result indicated that the oxidation reaction of MTX on the prepared sensor was a surface-controlled process. Meanwhile, the peak oxidation potential of MTX was also linearly related to the natural logarithm of the scan rate (ln$v$), and the linear equation was E_P (V)= 0.0286ln$v$+0.62098 (R^2=0.99824) (Fig.4C). Given that MTX behaved as a surface-controlled oxidation reaction on the AB/GCE electrode, the oxidation peak potential and scan rate satisfied the following equation [21]:

$$E_P = E^0 + RT/(\alpha nF)\ln[RTk^0/(\alpha nF)] + RT/(\alpha nF)\ln v$$

Where E^0 represents the standard potential; T represents the temperature; α represents the transfer coefficient and is frequently considered 0.5 in irreversible reactions; F represents the Faraday constant; and n and k^0 represent the electron transfer number and electron transfer rate constant, respectively. From the preceding equation, n=1.81. Therefore, the oxidation of MTX on the sensor was a two-electron and one-proton process controlled by the surface.

3.3. Analytical performance

The calibration curve obtained via CV under optimal conditions is shown in Fig.5A. The peak current was proportional to the MTX concentration by changing the concentration within the range of 0.005 μM to 3 μM. In Fig.5B, two linear relationships were found over the MTX concentration range of 0.005 μM to 3 μM, and these relationships can be presented by the following equations: I (μA)= 23.53054C (μM)+0.02067 (R^2=0.99155) within the range of 0.005 μM to 0.2 μM; and I (μA)= 11.30373C (μM)+2.79152 (R^2=0.99697) within the range of 0.2 μM to 3 μM. The limit of detection (LOD) of this method was 3.81 nM in accordance with 3*s*/*b*, where *s* is the relative standard deviation (RSD) of the cubic blank value, and *b* is the slope of the linear curve.

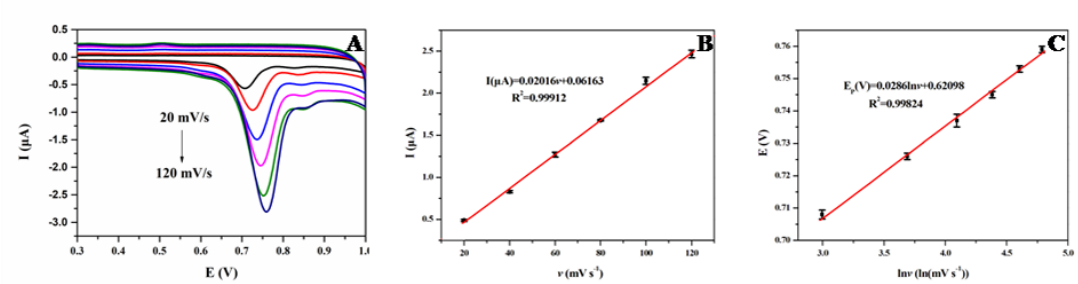

Figure 4. (A) CV curve of 0.1 μM MTX in PBS (0.1 M, pH6.0) on AB/GCE at different scan rates: 20, 40, 60, 80, 100, and 120 mV s^{-1}. (B) Linear relationship between peak current and scan rate. (C) Linear relationship between peak potential and the natural logarithm of the scan rate (ln*v*). The other conditions are the same as those in Fig.2.

Table 1 provides a comparison of the linear range and LOD obtained for MTX in this work with those reported literatures [27-29]. Compared with V_2O_5@g-C_3N_4/SPCE and WP/N-CNT electrode, this work displayed a lower LOD. And in comparation with PLL/GCE, which had a lower LOD for the detection of MTX, this method shown a wider linear range of 0.005-3 μM. In addition, the prepared sensor consumed less time and labor, was economical, and easy to operate. Therefore, the preparation of this electrode is quite necessary and important.

Table 1. Analytical performance of MTX electrochemical sensors

Sensors	Linear Range(μM)	Detection Limit(nM)	Reference
V_2O_5@g-C_3N_4/ SPCE	0.025–273.15	13.26	[27]
WP/N-CNT	0.01–540	45	[28]
PLL/GCE	0.005-0.2	1.7	[29]
AB/GCE	0.005-3	3.81	This work

g-C_3N_4: graphitic carbon nitride. V_2O_5: vanadium pentoxide. SPCE: screen-printed carbon electrode. N-CNT: nitrogen-doped carbon nanotube. WP: tungsten phosphide. PLL: poly (l-lysine). AB: acetylene black. GCE: glassy carbon electrode.

The repeatability and stability of the prepared AB/GCE were also tested. The RSD of six repeated experiments a day for 0.5 μM MTX was 4.82%. One electrode per day was prepared to determine MTX within 1 week, and the RSD of the peak current was 6.85%. Therefore, the prepared sensor exhibited satisfactory repeatability and stability.

3.4. Interference studies

Selectivity is a significant factor in the electrochemical sensor detection of MTX. In the current study, the effect of organic or inorganic substances on MTX detection was studied by adding different potential interfering substances into the buffer solution with 0.5 μM MTX. Non-interference was defined as a change of less than ±10% of the peak current of MTX detection in the current caused by potential interfering substances.

Table 2. Interference levels of several substances in determining 0.5 μM MTX

Substances	Interference Level
Na^+, K^+, Cl^-	500
Fe^{3+}, Fe^{2+}, Zn^{2+}, SO_4^{2-}	200
glycine, glucose, vitamin C	10
citric acid	5

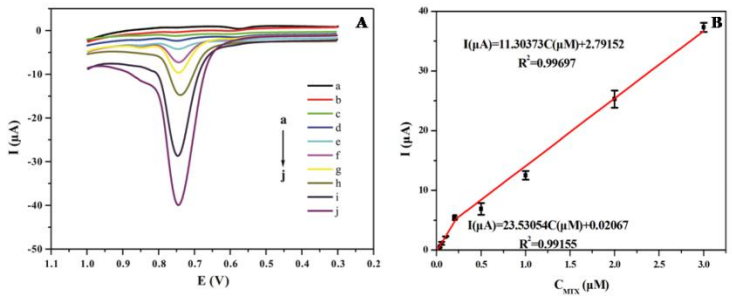

Figure 5. (A) CV curves of AB/GCE in different concentrations of MTX (from a to j): 0.005, 0.01, 0.02, 0.05, 0.1, 0.2, 0.5, 1, 2, and 3 μM. (B) Standard curve of MTX under the optimized conditions.

The results in the presence of 500-fold of Na^+, K^+, and Cl^-; 200-fold of Fe^{3+}, Fe^{2+}, Zn^{2+}, and SO_4^{2-}; 10-fold of glycine, glucose, and vitamin C; and 5-fold of citric acid are provided in Table 2. Thus, the prepared sensor exhibited satisfactory anti-interference for MTX detection.

3.5. Analytical application

The content of MTX in the human serum was detected using the prepared AB/GCE sensor.

Table 3. Determination of MTX in the human serum at AB/GCE

Sample	Added (μM)	Found (μM)	Recovery (%)	RSD (%) (n=3)
1	0.05	0.047	94.0	0.47
	0.1	0.092	92.0	0.12
	0.2	0.219	109.5	0.31
2	0.05	0.050	100.0	0.01
	0.1	0.096	96.0	0.29
	0.2	0.210	105.0	2.33

3	0.05	0.055	110.0	0.24
	0.1	0.099	99.0	0.07
	0.2	0.227	113.5	5.77

Table 3 shows that the recoveries of MTX in this work were within the range of 92-113.5%, indicating that the prepared sensor can be used in the accurate detection of MTX.

4. CONCLUSION

A novel electrochemical sensor with AB as modifier was prepared for determining MTX in clinical serum samples. The prepared sensor exhibited low LOD and good linear relationship for MTX detection. In addition, the proposed sensor demonstrated satisfactory selectivity, repeatability, and stability toward MTX. Thus, a practical platform for MTX determination in serum is presented.

CONFLICTS OF INTEREST
The authors declare no conflict of interest.

FUNDING
This research was funded by the China Postdoctoral Science Foundation (No. 2018M632629), Basic Research on the Application of Young Talents (No. 18-2-2-53-jch), the Natural Science Foundation of Shandong Province (No. ZR2019BH053).

AUTHOR CONTRIBUTIONS
All authors contributed significantly to this work.

ACKNOWLEDGMENTS
We thank all participants for their involvement in our study.

References

1. N. Oosterom, R. de Jonge, D. E. C. Smith, R. Pieters, W. J. E. Tissing, M. Fiocco and B. D. van Zelst, *PLoS One*, 14 (2019) e0221591.
2. N. Sakamoto, S. Hara, H. Ishimoto, S. Nakashima, H. Yura, T. Miyamura, D. Okuno, A. Hara, T. Kakugawa, H. Yamaguchi, Y. Obase, H. Kushima, H. Ishii, S. Noguchi, T. Kido, T. Kobayashi, Y. Soejima, S. Yoshioka, Y. Ishimatsu, K. Yatera, J. I. Kadota and H. Mukae, *Tohoku J Exp Med*, 248 (2019) 209-216.
3. E. E. W. Cohen, L. F. Licitra, B. Burtness, J. Fayette, T. Gauler, P. M. Clement, J. J. Grau, J. M. Del Campo, A. Mailliez, R. I. Haddad, J. B. Vermorken, M. Tahara, J. Guigay, L. Geoffrois, M. C. Merlano, N. Dupuis, N. Kramer, X. J. Cong, N. Gibson, F. Solca, E. Ehrnrooth and J. H. Machiels, *Ann Oncol,* 28 (2017) 2526-2532.
4. E. R. Plimack, J. H. Hoffman-Censits, R. Viterbo, E. J. Trabulsi, E. A. Ross, R. E. Greenberg, D. Y. Chen, C. D. Lallas, Y. N. Wong, J. Lin, A. Kutikov, E. Dotan, T. A. Brennan, N. Palma, E. Dulaimi, R. Mehrazin, S. A. Boorjian, W. K. Kelly, R. G. Uzzo and G. R. Hudes, *J Clin Oncol,* 32 (2014) 1895-1901.
5. S. C. Howard, J. McCormick, C. H. Pui, R. K. Buddington and R. D. Harvey, *Oncologist*, 21 (2016) 1471-1482.

6. J. C. Gutierrez and K. Hwang, *Expert Opin Drug Metab Toxicol*, 13 (2017) 51-58.
7. S. Padmanabhan, D. N. Tripathi, A. Vikram, P. Ramarao and G. B. Jena, *Mutat Res*, 655 (2008) 59-67.
8. J. N. Van der Beek, N. Oosterom, R. Pieters, R. de Jonge, M. M. van den Heuvel-Eibrink and S. G. Heil, *Crit Rev Oncol Hematol*, 142 (2019) 1-8.
9. E. den Boer, S. G. Heil, B. D. van Zelst, R. J. Meesters, B. C. Koch, M. L. Te Winkel, M. M. van den Heuvel-Eibrink, T. M. Luider and R. de Jonge, *Ther Drug Monit*, 34 (2012) 432-439.
10. D. Wu, Y. Wang, Y. Sun, N. Ouyang and J. Qian, *Biomed Chromatogr*, 29 (2015) 1197-1202.
11. M. Montemurro, M. M. De Zan and J. C. Robles, *J Pharm Anal*, 6 (2016) 103-111.
12. E. Begas, C. Papandreou, A. Tsakalof, D. Daliani, G. Papatsibas and E. Asprodini, *J Chromatogr Sci*, 52 (2014) 590-595.
13. D. Kim, J. Han and Y. Choi, *Anal Bioanal Chem*, 405 (2013) 377-387.
14. S. Tesfalidet, P. Geladi, K. Shimizu and B. Lindholm-Sethson, *Anal Chim Acta*, 914 (2016) 1-6.
15. S. Chen, Z. Zhang, D. He, Y. Hu, H. Zheng and C. He, *Luminescence*, 22 (2007) 338-342.
16. Z. Zhu, H. Wu, S. Wu, Z. Huang, Y. Zhu and L. Xi, *J Chromatogr A*, 1283 (2013) 62-67.
17. D. Sun and H. Zhang, *Water Res*, 40 (2006) 3069-3074.
18. W. Xu, F. Yuan, C. Li, W. Huang, X. Wu, Z. Yin and W. Yang, *J Sep Sci*, 39 (2016) 4851-4857.
19. S. Tang, H. Shen, Y. Hao, Z. Huang, Y. Tao, Y. Peng, Y. Guo, G. Xie and W. Feng, *Biosens Bioelectron*, 104 (2018) 72-78.
20. Y. Zhang, Y. Wang, K. Wu, S. Zhang, Y. Zhang and C. Wan, *Colloids Surf B Biointerfaces*, 103 (2013) 94-98.
21. Q. Cheng, Y. Du, K. Wu, J. Chen and Y. Zhou, *Colloids Surf B Biointerfaces*, 84 (2011) 135-139.
22. X. Hu, P. Wang, J. Yang, B. Zhang, J. Li, J. Luo and K. Wu, *Colloids Surf B Biointerfaces*, 81 (2010) 27-31.
23. X. Yang, M. Gao, H. Hu and H. Zhang, *Phytochem Anal*, 22 (2011) 291-295.
24. H. Zhang, C. Hu, W. Lan and S. Hu, *Anal Bioanal Chem*, 380 (2004) 303-309.
25. X. Wei, Q. Zhao, W. Wu, T. Zhou, S. Jiang, Y. Tong and Q. Lu, *Sensors (Basel)*, 16 (2016) 1539.
26. X. Yang, H. Qin, M. Gao and H. Zhang, *J Sci Food Agric*, 91 (2011) 2821-2825.
27. T. W. Chen, U. Rajaji, S. M. Chen, B. S. Lou, N. Al-Zaqri, A. Alsalme, F. A. Alharthi, S. Y. Lee and W. H. Chang, *Ultrason Sonochem*, 58 (2019) 104664.
28. H. Zhou, G. Ran, J. F. Masson, C. Wang, Y. Zhao and Q. Song, *Biosens Bioelectron*, 105 (2018) 226-235.
29. Y. Wei, L. Luo, Y. Ding, X. Si and Y. Ning, *Bioelectrochemistry*, 98 (2014) 70-75